Chinese Science Bulletin



# Changes in sea surface temperature in western South China Sea over the past 450 ka

LI Li†, WANG Hui, LI JianRu, ZHAO MeiXun & WANG PinXian

State Key Laboratory of Marine Geology, Tongji University, Shanghai 200092, China

**Sea surface temperature over the past 450 ka was obtained by the unsaturation of molecular fossil-long chain alkenone with a resolution of about 1 ka from the western South China Sea. This is the longest temperature profile in the South China Sea at such high resolution. The $U_{37}^{k'}$-SST results revealed similar glacial-interglacial cycles as the $\delta^{18}O$ profile of planktonic foraminifera, with SST variability of 23—25.5℃ for glacial and 25—28℃ for interglacial periods. The highest SST (28.4℃) was recorded at MIS5.5 and lowest SST (22.6℃) during MIS2. The SST record preceded the planktonic foraminiferal $\delta^{18}O$ on five glacial-interglacial transitions. Comparison of temperature records from the Southern and Northern Hemispheres indicated a more Southern Hemisphere-like pattern for the temperature variation in the SCS. Strong precession and semiprecession signals in the spectra of our SST record manifest the tropical phenomena.**

sea surface temperature, unsaturation of long chain alkenone, South China Sea, paleoclimate, late Quaternary



In the late 1970s, the CLIMAP program projected no remarkable change in sea surface temperature (SST) in middle and low latitudes during the last glacial maximum (LGM) by using foraminifera transfer function[1], making a misimpression that the tropic region was insensitive to climate change during the glacial/interglacial cycle. Only a decade ago, Thunell et al.[2] considered that SST in the tropic Pacific did not change much in the last glacial-interglacial cycle using the modern analog technique on foraminifera. Because not all the planktonic foraminifera used in these estimates lived in the sea surface and their assemblages were affected by many different environmental factors, it is always difficult to get the precise temperature information no matter which paleoecological method is used. With the development of analytical techniques over the years, reconstruction of the SST has extended from paleoecology into geochemistry methods, among which the $U_{37}^{k'}$-SST and the Mg/Ca-SST methods have been widely used for paleotemperature reconstructions.

The South China Sea (SCS), the largest marginal sea in the western Pacific, has recently become an international focal point in paleoceanographical studies. Many researchers had tried to reconstruct SST variations in the SCS using different kinds of methods. Results from Mg/a-SST[11–14] and $U_{37}^{k'}$-SST[15–21] techniques appear to be more reliable than those from other methods in reconstructing SST, although methods based on planktonic foraminiferal assemblages are still being used[8–10]. However, the time span for most SST records generated by $U_{37}^{k'}$ and Mg/Ca techniques in the SCS is relatively short, with the longest being only for the last 260 ka[11]. In this study, we used $U_{37}^{k'}$ method to reconstruct SST variability in the western SCS off Vietnam for an extended sequence over the past 450 ka. We will also discuss the differences between various SST methods and between the lower and higher latitudes, as well as the

Received March 28, 2008; accepted December 11, 2008; published online April 5, 2009
doi: 10.1007/s11434-009-0083-9
†Corresponding author (email: lilitju@tongji.edu.cn)
Supported by the National Natural Science Foundation of China (Grant Nos. 40403012 and 40621063), Program for Young Excellent Talents in Tongji University (Grant No. 2006KJ055), National Basic Research Program of China (Grant No. 2007CB815904) and Shanghai Rising-Star Program (A) (Grant No. 08QA14065)

**Citation:** Li L, Wang H, Li J R, et al. Changes in sea surface temperature in western South China Sea over the past 450 ka. Chinese Sci Bull, 2009, 54, 3335—3343, doi: 10.1007/s11434-009-0083-9

SST characterization of the tropic region in glacial- interglacial cycles.

## 1 Materials and methods

Core MD05-2901(14°22.50′N, 110°44.60′E, w.d. 1454 m, core length 3649 cm) was retrieved during IMAGE XII cruise through a Chinese-French cooperation venture in 2005 (Figure 1). Samples were taken at 8-cm intervals except between 1365 cm and 1435 cm where no sample was collected because of severe disturbance of the ship during coring.

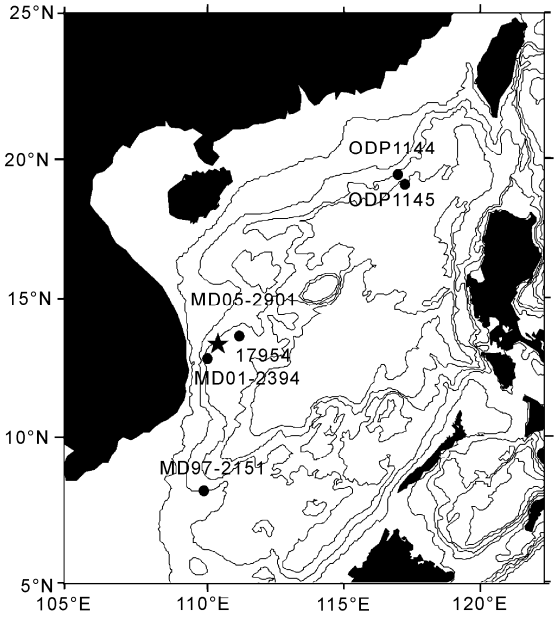


**Figure 1** Location of site MD05-2901. ★ represents the site in this study and ● other SCS sites mentioned in this article.

High-resolution oxygen isotope stratigraphy. Stable isotopic measurement was done on planktonic foraminifer *Globigerinoides ruber* with shell size of 0.25－0.30 mm using a mass spectrometer MAT252 (Finnigan, Thermo Electron) with an auto carbonate device (Kiel III). The instrumental standard deviation is 0.08‰. The age model for this core was generated by comparison with the complied $\delta^{18}$O curve by Shackleton[22], and further constrained by the first and last appearance events of the pink *G. ruber* at 407 ka and 125 ka, respectively[23]. The finial depth-age correlation was obtained by linear insert. According to this age model, the bottom age of the core is 447 ka, and the 8-cm sampling intervals correspond to ~1 ka temporal resolution. Detailed measurement and age controlling points can be found in Ref. [23].

$U^{k'}_{37}$-SST measurement. About 2－3 g freeze-dried samples were extracted ultrasonically four times by dichloromethane/methanol (3∶1, *V/V*), after adding an internal standard. The extracts were concentrated (3000 r/min, 5 min) and then saponified with 3 mL of 6% KOH/methanol overnight. Neutral components were recovered by extraction with *n*-hexane four times, then separated into alkanes and alcohols by silica gel column. Alkenones within the alcohol subfraction were analyzed by gas chromatography after derivitization by N, O-bis (trimethylsily)-trifluoroacetamide (BSTFA) (70℃, 2 h).

Gas chromatography (GC) measurement. GC was performed on a Trace GC 2000 chromatography (Finnigan, Thermo Electron) equipped with HP-1 capillary column (50 m × 0.32 mm × 0.17 μm, J&W) and flame ionization detector. Both the injector and detector were set at 300℃. Helium was used as the carrier gas with a flow rate of 1.2 mL/min by splitless injecting. The oven was kept initially at 60℃ for 1 min, then was programmed from 60℃ to 200℃ at 20℃/min, followed by 5℃/min to 270℃, then 1.3℃/min to 300℃ (maintained for 18 min), 5℃/min to 310℃ (maintained for 5 min). The standard deviation for $U^{k'}_{37}$ method is 0.006, corresponding SD for SST estimation in this study is < 0.2℃.

MS operation. EI ion source with temperature of 200℃ and emission electron energy of 70 eV, mass range of *m/z* 50－600, connecting temperature of 300℃) (Trace DSQ, Finnigan, Thermo). GC/MS and alkenone standards were also used for the retention time to confirm alkenones without co-eluting existence.

## 2 Results

Two kinds of $C_{37}$ alkenones ($C_{37:2}$, $C_{37:3}$) existed in the western SCS sediment, although the content of $C_{37:3}$ alkenone was relatively low. The highest $U^{k'}_{37}$ value is 0.973 and the lowest 0.792. From our observation, the fluctuation of $C_{37}$ alkenones during the past 450 ka was not caused by post-depositional diagenesis or by microbial degradation because these processes tend to result in uniform variation for the detected alkenones (data not published).

Although *E. huxleyi* is the dominant alkenone producer in the modern ocean, some studies show that paleotemperature similar to those estimated from the foraminiferal $\delta^{18}$O can be obtained according to the $U^{k'}_{37}$-

SST equation[24] using surface sediments even when *E. huxleyi* is low or absent, or coccolithophorid assemblages undergo a major change[25]. This indicates the wide applicability of the $U^{k'}_{37}$-SST equation. Our results show almost identical SST using different $U^{k'}_{37}$-SST experimental equations[19,24]. In this study, we mainly present results using the equation of Pelejero and Grimalt ($U^{k'}_{37}$ = 0.031×SST+0.092)[19] for estimating the SST variability in the western SCS during the past 450 ka. As shown in Figure 2, the temperature in the core top is 27.7℃, which is consistent with the average annual temperature of ~27.4℃ by modern observation[26] and close to the annual mean temperature of 27.2℃ in 0—30 m water depth reported by Pelejero[19]. Overall, the estimated SST for the western SCS varied in a range of 22.6—28.4℃, with typical glacial/interglacial alternations over the past 450 ka.

For the five interglacial periods, the SST varied between 24.5℃ and 28℃. The highest interglacial SST (28.4℃) is recorded for MIS5.5 (121.3 ka) and the lowest SST (23.4℃) for MIS7.4 (224.8 ka). This 5℃ temperature amplitude is similar to the glacial-interglacial amplitude, implying unstable climate during these interglacial periods.

The estimated SST for the five glacial periods (MIS2-4, 6, 8, 10, 12) varied mainly in a range of 25.5—23.5℃ with relatively lesser fluctuations in amplitude (except MIS8.5) compared with that in interglacials. The lowest glacial temperature of 22.6℃ appeared in MIS 2 (18.6 ka) while abnormally high temperature of ~26℃ was found in MIS 8.5 (286.6 ka). Similarly high SST during MIS 8 had been found in core FR1/94-GC3 from the Tasman Sea using $U^{k'}_{37}$-SST[27], at ODP 806 in the west Pacific using Mg/Ca-SST[28], and at ODP 723 in the Arabian Sea using $U^{k'}_{37}$-SST[29]. Meanwhile, the $U^{k'}_{37}$-SST record from core MD97-2120 in the northwest Pacific shows lower SST in MIS 8.5 than in MIS 7.5 but close to MIS 7.1 and 7.3. All these indicate that the abnormally high temperature in MIS 8.5 is a worldwide phenomenon. SST estimations of core MD97-2142 by foraminiferal transfer function also showed warm events during MIS 6, 8, and 12, implying that the sea surface temperature was influenced by many factors rather than by ice sheet driving only[10].

Among the five glacial/interglacial transitions, Termination II (MIS6/5) was absent from this study because of the lack of samples and the other four Terminations (I and III—V) showed different patterns of temperature change. The largest glacial/interglacial SST difference occurred in Termination I (MIS2/1), which was up to 5.2℃ This was followed by 4.7℃ difference for Termination V (MIS12/11), 3.5℃ difference for Termination III (MIS8/7), and 3.1℃ difference for Termination IV (MIS10/9). Among these four transitions, SST increase (averaging 0.4℃ /ka) across Termination V was most rapid as marked by temperature increase from 23.1℃ at 435.4 ka to 27.8℃ at 423.5 ka. Several several dramatic warming episodes also occurred during this transition. The average rate of SST increase for Terminations I, III and IV is 0.35, 0.3, 0.32℃/ka, respectively, accompanied by various amplitudes in temperature fluctuation except the relatively gentle increase in Termination IV.



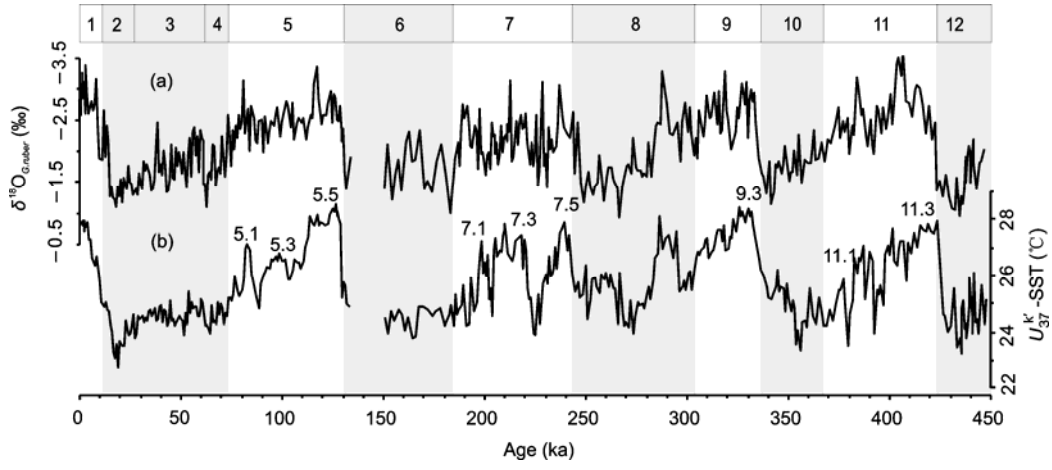


**Figure 2** $\delta^{18}$O curve of planktonic foraminifera *G. ruber* (a) and $U^{k'}_{37}$-SST curve (b) in core MD05-2901.

## 3 Discussion

### 3.1 Comparison between the $U_{37}^{k'}$-SST and foraminiferal oxygen isotope record

For the past 450 ka, the $U_{37}^{k'}$-SST record was almost synchronous with foraminiferal oxygen isotope curve in core MD05-2901, with heavier $\delta^{18}O$ values corresponding to lower temperatures and lighter $\delta^{18}O$ values to higher temperatures (Figure 2). Detailed comparison reveals that increases in SST slightly precede the depletions of $\delta^{18}O$ during glacial/interglacial transitions. Especially, the warming time in Termination IV was about 13 ka earlier than the depletion of $\delta^{18}O$ in *G. ruber*. SST leading $\delta^{18}O$ by more than 10 ka has been reported from the northern Atlantic due to the regional reduction of the California Current[31]. Similar phenomenon has also been found in the Mg/Ca-SST record from the west Pacific[28].

In Terminations I, III and V, the rises of SST led the lows of $\delta^{18}O$ values by about 0.6 ka, 2 ka, 0.4 ka, respectively. Generally, foraminiferal $\delta^{18}O$ mainly records the ice sheet information. Our results indicate that SST in the low latitude marginal sea increased before the ice sheet melting. Previous studies also show that SST led the reduction of ice volume represented by the foraminifera $\delta^{18}O$, such as the rising in Mg/Ca-SST preceded ice sheet decay by about 2−3 ka in the western Pacific warming pool[28,32] and by 3.5 ka in the Sulu Sea[32]. During the last deglaciation warming, Mg/Ca-SST also preceded the oxygen isotope change at ODP1144 in the northern SCS[11]; the pollen composition records from the same site also showed a warming by 2.5 ka earlier than in high latitudes[34]. High-resolution sediment research in Lake Huguang Maar also implied earlier warming in lower latitude than in higher latitude of the Northern Hemisphere[35]. However, some studies indicate synchronous temperature change in lower latitudes with ice volume[12,16,36,37]. For example, Mg/Ca-SST indicating deglacial warming at ODP 1145 in the northern SCS was after the ice sheet decay, but nearly synchronous during the penultimate deglaciation[12]. However, the influence of differential post-deposition dissolution of foraminifera in ODP1145 samples should not be overlooked according to Wei et al.[11]. Although there is no unanimous opinion whether the low latitude SST indeed preceded $\delta^{18}O$ at glacial/interglacial transitions, a likely lead of temperature over the ice sheet decay, as revealed by the present and previous studies cited above, may have been caused by changes in hydrological cycles in the tropical ocean[34]. SST was mainly influenced by air circulation which moved relatively faster than water circulation. The latter was controlled by ice volume and recorded in foraminiferal $\delta^{18}O$.

In spite of the general coherence between $U_{37}^{k'}$-SST and $\delta^{18}O_{G.\ ruber}$ records, some divergence also existed such as the signal for the Younger Dryas event with about 0.7‰ positive shift in $\delta^{18}O$, which is significantly above the analytical error (0.08‰); but $U_{37}^{k'}$-SST decrease only by 0.2℃, which is close to the analytical error. Similar phenomena have been observed in nearby cores using the $U_{37}^{k'}$-SST method. $U_{37}^{k'}$-SST may not reveal clearly as the $\delta^{18}O_{G.\ ruber}$ record the YD event on the millennial resolution[18]. Similarly, some high-resolution $U_{37}^{k'}$-SST records indicate the YD event, but those low resolution $U_{37}^{k'}$-SST records do not. The YD event has been found very clearly in cores 17940, 18287 and 18252 (resolution of 0.2−0.3 ka). The YD event is detectable in core 17964 (resolution of 0.5 ka), but is completely obscure in cores 17961 and 17954 (resolution of 1.1 ka and 1.7 ka, respectively)[16,18]. A compilation of 90 sites in the Pacific by Kiefer and Kienast indicated that the absence of rapid climate events such as the YD event in lower resolution and/or lower sedimentation rate sites may be due to the unresolved SST variability or bioturbational attenuation of the signal[39]. On the other hand, the absence of rapid climate events from sites with high enough resolution and sedimentation rates, especially in the equatorial western Pacific, suggested that the change in the intensity of meridional overturning circulation (MOC) and atmospheric circulation associated with the millennial-scale events did not influence these regions[39]. These differences in SST and $\delta^{18}O$ records can also be found in other periods, such as in late MIS 5.5 (117.3 ka), MIS 7.4 (228 ka) and MIS 11.3 (404−408 ka). At MIS 5.5, the $\delta^{18}O$ values depleted from –2.56‰ to –3.36‰ but the SST remained relatively stable (Figure 2).

In addition, the SST was controlled by the ocean-air exchange while foraminiferal $\delta^{18}O$ values are affected not only by temperature but also by the sea water $\delta^{18}O$ (including the ice sheet effect and salinity effect). A detailed study demonstrated lower sea surface salinity (SSS) in periods with remarkablly depleted foraminiferal $\delta^{18}O$, implying an integrated action of global and

regional factors[38], such as ice sheet melting, sea level rising, and local precipitation, fluvial discharge and evaporation. The absence of the millennial-scale events (such as YD, B-A events) in the high-resolution SST record from the Sulu Sea may be primarily due to changes in salinity[33].

### 3.2 SST comparison between different SCS sites

Five detailed SST profiles over the past 270 ka showed similar variations. These include $U^{k'}_{37}$-SST for core MD05-2901 (this study), core 17954[18] nearby and core MD97-2151[15] from the southern SCS, and Mg/Ca-SST for ODP 1144[11] and ODP 1145[12] from the northern SCS (Figure 3). More than 5℃ temperature gradient between the last glacial maximum (LGM) and Holocene was found in four SST records and －4℃ for the southern core MD97-2151. MIS 5.5 temperature was higher than in the Holocene although the ODP 1144 record is not clear because MIS 5.5 is absent. These results differ greatly with the CLIMAP estimates that SST from the last glacial to Holocene changed little in the tropics[1]. The lowest SST was found in MIS2 of all records except for core MD97－2151. During MIS 5.4, two cold events can also be found in all these records[12,15].

Higher SST values, larger fluctuation amplitude, higher frequency variability in the Mg/Ca-SST estimates from the northern SCS than the $U^{k'}_{37}$-SST record from the southern SCS could be due to higher sensitivity, higher analytical noise and/or higher inherent errors in the Mg/Ca-SST method[38]. The differential bioturbational mixing of alkenone from coccolithphorides and foraminifera may be an alternative reason for the relatively smoother $U^{k'}_{37}$-SST record[40].

SST estimated using the modern analog technique for the western SCS also exhibit annual variation in average temperature, which is consistent with the $U^{k'}_{37}$-SST record (23.5－28.5℃) but lacking an obvious glacial/interglacial pattern shown in the $U^{k'}_{37}$ and Mg/Ca results. In comparison with those obtained by paleothermal methods of $U^{k'}_{37}$ and Mg/Ca, SST estimated by the paleoecology statistics exhibits its more errors due to different living modes and preservation of foraminifera. In many cases, SST reconstructions by faunal assemblage meth-

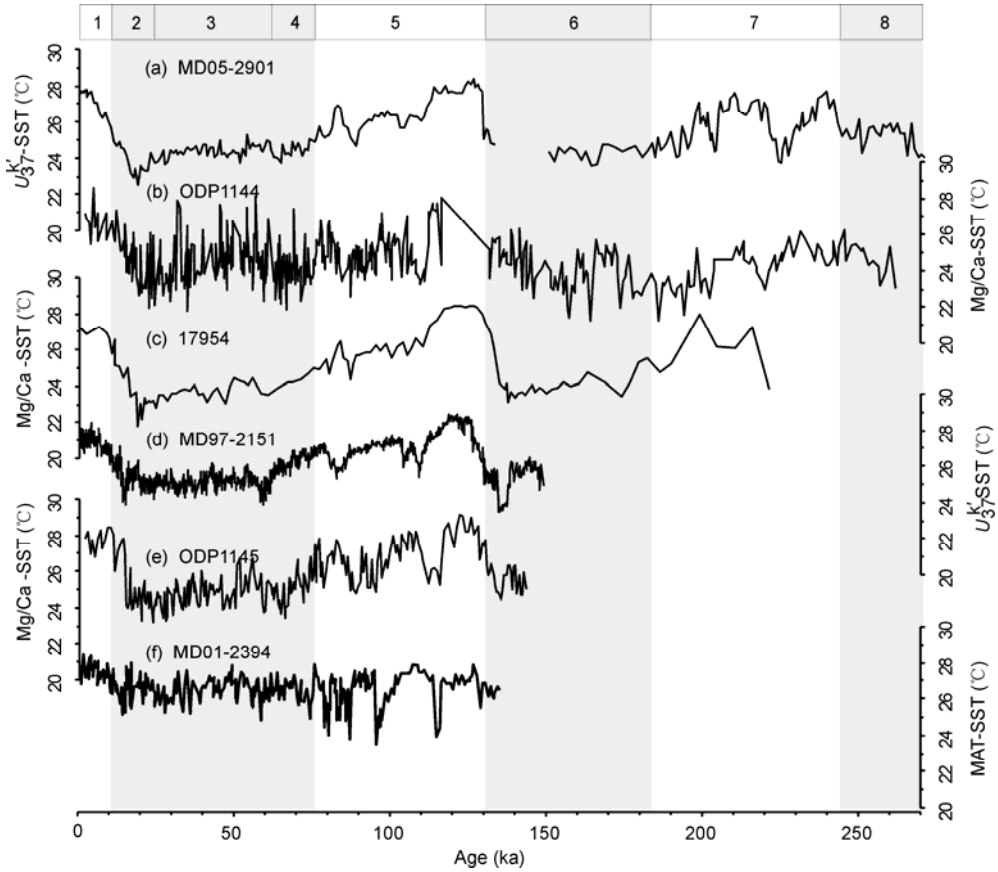


**Figure 3** Comparison of the high-resolution SST records at different sites in the South China Sea (see Figure 1 for their locations).

ods show no clear glacial cycles but some times even higher temperature in glacial periods than in interglacial periods[8–10,41].

Moreover, paleotemperature reconstruction was also influenced by other ecological properties of foraminifera and nannoplanktons, including different seasons for species breeding and shell growing, as well as the species diversity in the water column. In the eastern SCS, SST for MIS 11 based on foraminifera transfer function shows no obvious temperature oscillations[8]; however, a 4—5℃ difference for the same period is found in core MD05-2901 from the western SCS using the $U_{37}^{k'}$ method (Figure 2) and there appears to be times associated with sudden decreases in temperature. Based on different living modes of the coccolithphorides (the alkenone producer) and planktonic foraminifera, Pflaumann and Jian[42] believed that SST estimates using the $U_{37}^{k'}$ method and foraminiferal assemblage represent temperature variations in the euphotic zone and in the entire upper water column, respectively. However, the uncertainty in faunal estimates may also be attributed to large deviations between the two methods because of the limited number and diversity of reference samples from the Pacific[39]. In addition, SST estimates by unsaturation of the long chain alkenones produced by coccolithphorides possibly reflect temperature in the maximum coccolithphorides productivity, i.e. the $U_{37}^{k'}$-SST likely corresponds to the temperature of coccolithphorides bloom season, which is in late spring and early summer in the subtropical eastern Atlantic, in summer in the Sea of Japan, in autumn and winter in the northern SCS[20,45,46], and in early summer near the Okinawa Trough although a winter bloom at the last locality had been reported in an early study[47–49] . However, $U_{37}^{k'}$-SST may actually represent the mean annual temperature in tropical-temperate zones[24,50], such as the results shown by Pelejero and Grimalt[19] for core-top sediments from the SCS. Because information on the coccolithphoride ecology in this region is absent, the $U_{37}^{k'}$-SST record in this study can be taken as representing the annual average temperature following Pelejero and Grimalt[19], although the record shows a closer resemblance to the winter temperature in the northern SCS[20,46].

### 3.3 Latitudinal SST comparisons

SST records from various latitude regions show two cooling patterns during the glacial/interglacial cycles (Figure 4). One pattern is the Antarctic pattern characterized by relatively stable SST after a high temperature period at early interglacials (MIS11.3, 9.3, 7.5, 5.5) except for MIS7. The other is the Northern Hemisphere pattern characterized by gradual cooling from the early glacial high temperature to the lowest temperature in glacial maxima interrupted by several dramatic cooling episodes, such as the Heinrich events or analogies. Moreover, deglacial warming in the Southern Hemisphere appears to occur prior to that in the Northern Hemisphere (Figure 4). At Termination IV with the closest warming time between the two hemispheres, warming in the Southern Hemisphere still led that in the Northern Hemisphere by at least 2 ka. More dramatic and fast warming occurred in the Northern Hemisphere than in the Southern Hemisphere but the temperature maxima were reached almost synchronically for both hemispheres. Different temperature variation patterns also existed before MIS10: two similarly cold periods at 358 ka and 345 ka in the Antarctic record, a two-step-warming in the western Pacific warming pool and South China Sea, but a one-step warming from 345 ka in the mid-latitude Northern Hemisphere with cooling at 358 ka, which was contrary to the warming trend in the Southern Hemisphere in the same period with a lag of warming by 3 ka. The warming of the SCS seems to lie in between south and north high latitude variations, implying a warming tendency from south to north. Recent research has shown that the Antarctic water mass joined the global thermohaline circulation through the convection exchange with the global ocean by surface, intermediate and bottom water masses, and was therefore further linked with the global climate. Especially, the Antarctic intermediate water (AAIW) plays an important role in the distribution of heat and fresh water in the upper water[54]. The warming trend from south to north during cold to warm transitions by temperature comparison between the low and high latitudes may have resulted from the heat transformation from south to north by the AAIW.

In general, the SST variability pattern from the SCS is similar to the pattern in the Southern Hemisphere, especially the lower SST in MIS7.4 (equivalent to values at the last glacial) and the higher SST in MIS 8.5 (equivalent to values at MIS 7.3). In contrast, the SCS foraminiferal $\delta^{18}O$ displayed a similar pattern with the northern high latitude, indicating stronger influence by the ice sheet in the northern high latitude. Similarly, the temperature record from the Sulu Sea also exhibited a

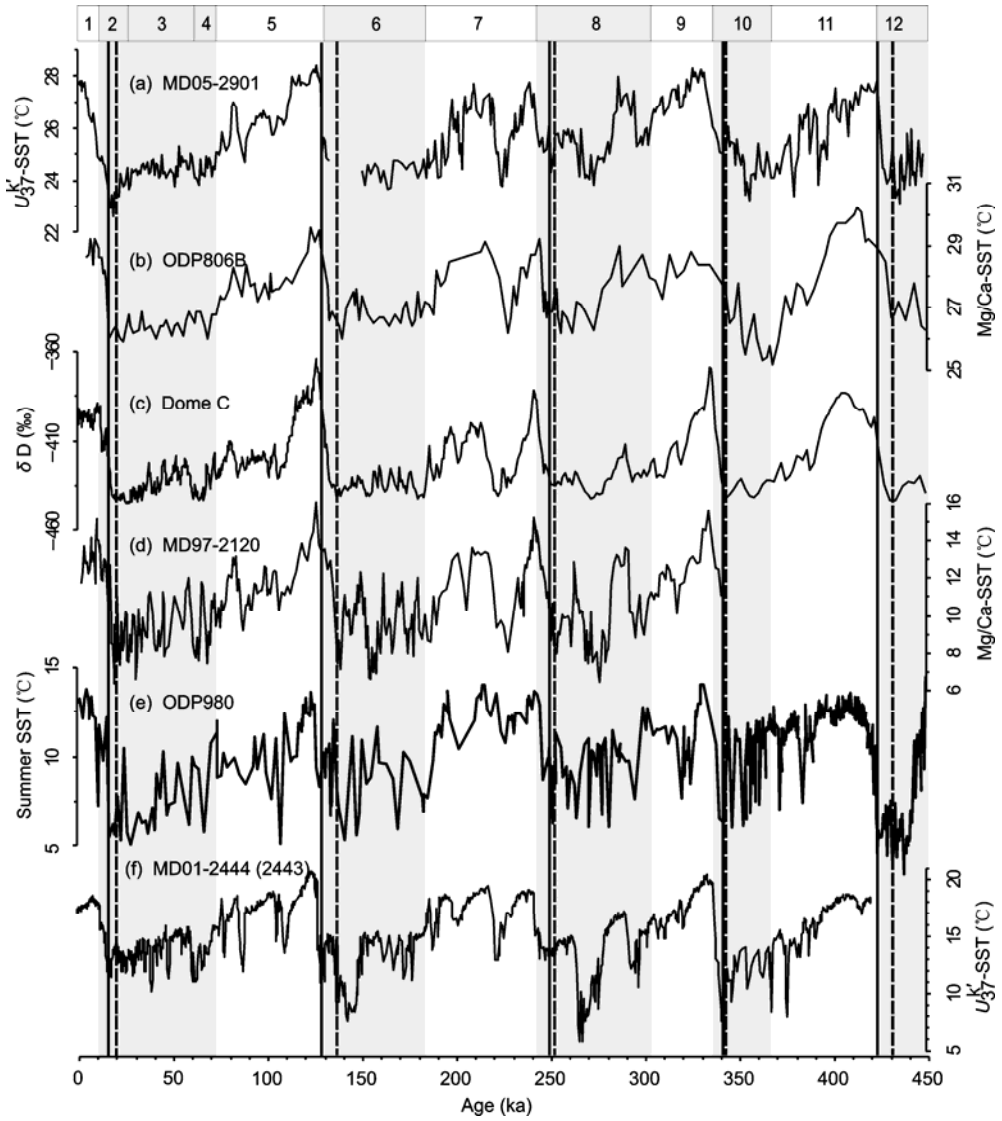


**Figure 4** Latitudinal SST comparisons during the past 450 ka. Dashed line represents the lowest temperature time in Antarctic and sold line represents that in high latitude in the Northern Hemisphere during the glacial/interglacial transition.

coupling with the Southern Hemispheric climate change, while the salinity record seemed to have been impacted mainly by the northern high latitude climate[36,55]. Although the link between the air temperature in Antarctica and the low latitude SST is still a puzzle, the SST variability pattern in the low latitude presented here challenges the traditional view that the ice sheet in the northern high latitude acted as the global climate trigger through the "ocean conveyer", implying the important role of low latitude in the global climate changes[56].

### 3.4 Spectrum analysis

The spectrum analysis of $U_{37}^{k'}$-SST revealed several dominant Milankovitch cycles (Figure 5): eccentricity cycle at 110 ka, obliquity cycle at 41 ka, precession cycle at 23 ka and semiprecession cycle at 11 ka. In comparison with the orbital cycles of SST, the spectrum analysis of foraminiferal $\delta^{18}$O displays periodicities at 75 ka, 56 ka and 26.5 ka besides the typical orbital cycles, implying the salinity effect on the $\delta^{18}$O change in addition to temperature effect. Obliquity periodicity is the result of the responding of the ice sheet at high latitudes to the orbital parameters. Therefore, the 41 ka periodicity of the $\delta^{18}$O and the SST indicate the impact of the high latitude on the low latitude climate. The sun radiates over the equator twice per year on vernal and autumnal equinox, respectively, producing the semiprecession cycle of about 10 ka. So, precession and semiprecession periodicities represent the response of the low latitude to the orbital driving. The distinct pre-

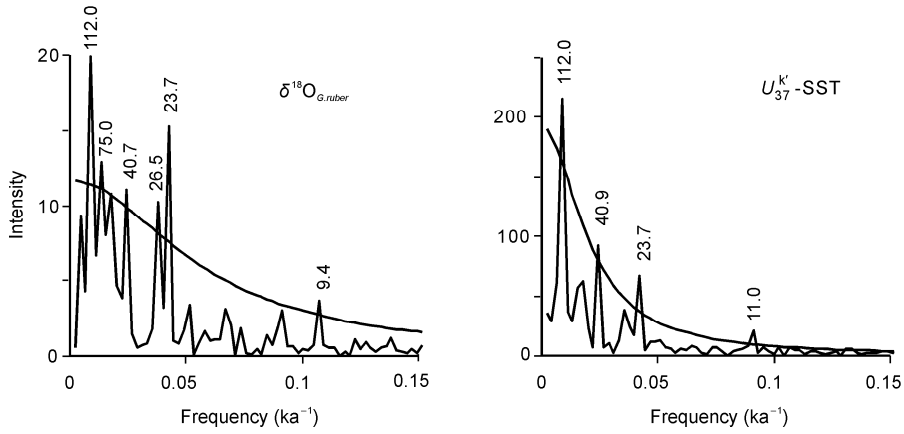


**Figure 5** Spectrum analysis of $\delta^{18}O_{G.ruber}$ and $U_{37}^{k'}$-SST in MD05-2901. The number in the figure corresponds to the periods (ka), real line represents confidence degree of 90% (Redfit analysis software[57]).

cession and semiprecession cycles of the foraminiferal $\delta^{18}O$ and SST in core MD05-2901 imply the tropical feature.

## 4 Conclusions

The $U_{37}^{k'}$-SST record from the western SCS exhibited typical glacial/interglacial cycles during the past 450 ka with mean amplitude of 4℃. During glacial/interglacial transition periods, SST increased prior to the foraminiferal $\delta^{18}O$. A good correlation exists in the SST record from different latitudes between the Northern and Southern Hemispheres, showing a transitional pattern from south to north. The SST change in the SCS is more similar to the pattern of the Southern Hemisphere. Typical Milankovitch periods appeared in the spectrum analysis of the foraminifera $\delta^{18}O$ and SST records. Strong precession and semiprecession cycles characterize the tropical feature.

*The authors thank French Polar Institute (IPEV) for their technique in retrieving samples during the IMAGES XII, MD-147-Marco Polo cruise. The reviewers are also thanked for their helpful suggestions.*

1 CLIMAP Project Members. The surface of the ice-age Earth. Science, 1976, 191: 1131－1137
2 Thunell R, Anderson D, Gellar D, et al. Sea surface temperature estimates for the tropical Western Pacific during the Last Glaciation and their implications for the Pacific warm pool. Quat Res, 1994, 41: 255－264
3 Brassell S C, Eglinton G, Marlowe I T. Molecular stratigraphy: a new tool for climatic assessment. Nature, 1986, 320: 129－133
4 Nürnnberg D, Bijma J, Hemleben C. Assessing the reliability of magnesium in foraminiferal calcite as a proxy for water mass temperatures. Geochim Cosmochim Ac, 1996, 60: 803－814
5 Wang P X, Wang L J, Bian Y H, et al. Late Quaternary paleoceanography of the South China Sea:Surface circulation and carbonate cycles. Mar Geol, 1995, 127: 145－165
6 Miao Q, Thunell R C, Anderson D M. Glacial-Holocene carbonate dissolution and sea surface temperature in the South China and Sulu Seas. Paleoceanography, 1994, 9: 269－290
7 Wang L J, Wang P X. Late Quaternary paleoceanography of the South China Sea: glacial-interglacial contrasts in an enclosed basin. Paleoceanography, 1990, 5: 77－90
8 Yu P S, Huang C C, Chin Y M, et al. Late Quaternary East Asian Monsoon variability in the South China Sea: Evidence from planktonic foraminifera faunal and hydrographic gradient records. Palaeogeogr, Palaeoclimatol Palaeoecol, 2006, 236: 74－90
9 Chen M T, Huang C C, Pflaumann U, et al. Estimating glacial western Pacific sea-surface temperature: methodological overview and data compilation of surface sediment planktic foraminifer faunas. Quat Sci Rev, 2005, 24: 1049－1062
10 Chen M T, Shiau L J, Yu P S, et al. 500000-year records of carbonate, organic carbon, and foraminiferal sea-surface temperature from the southeastern South China Sea (near Palawan Island). Palaeogeogr Palaeoclimatol Palaeoecol, 2003, 197: 113－131
11 Wei G J, Deng W F, Liu Y, et al. Higher-resolution sea surface temperature record derived from Foraminifera Mg/Ca ratios during the last 260 ka in the Northern South China Sea. Palaeogeogr Palaeoclimatol Palaeoecol, 2007, 250: 126－138
12 Oppo D W, Sun Y B. Amplitude and tuning of sea surface temperature change in the northern South China Sea: Dynamic link to the East Asian monsoon. Geology, 2005, 33: 785－788
13 Steinke S, Chiu H-Y, Yu P-S, et al. Mg/Ca ratios of two Globigerinoides ruber (white) morphotypes: Implications for reconstructing past tropical/subtropical surface water conditions. Geochem Geophys Geosy, 2005, 6: doi:10.1029/2005GC000926
14 Whitko A N, Hastings D W and Flower B P. Past sea surface temperatures in the tropical South China Sea based on a new foraminiferal Mg calibration. MAR Sci, 2002, doi: 01.020101
15 Zhao M X, Huang Ch-Y, Wang Ch-CH, et al. A millennia $U_{37}^{k'}$-sea-surface temperature record from the South China Sea over the last 150 kyr: Monsoon and sea-level influence. Palaeogeogr Palaeoclimatol Palaeoecol, 2006, 236: 39－55
16 Kienast M, Steinke S, Stattegger K, et al. Synchronous tropical South China Sea sea surface temperature change and Greenland warming during deglaciation. Science, 2001, 291: 2132－2134
17 Steinke S, Kienast M, Pflaumann U, et al. A high resolution sea-surface temperature record from the tropical South China Sea (16500－3000 yr B.P.). Quat Res, 2001, 55: 352－362

18 Pelejero C, Grimalt J O, Heilig S, et al. High resolution $U^{k'}_{37}$-temperature reconstructions in the South China Sea over the last 220 kyr. Paleoceanography, 1999, 14: 224－231
19 Pelejero C, Grimalt J O. The correlation between the $U^{k'}_{37}$ index and sea surface temperatures in the warm boundary: the South China Sea. Geochim Cosmochim Ac, 1997, 61: 4789－4797
20 Huang C Y, Wu S F, Zhao M X, et al. Surface ocean and monsoon climate variability in the South China Sea since last glaciation. Mar Micropaleontol, 1997, 32: 71－94
21 Huang C Y, Wu S F, Zhao M X, et al. Deep sea and lake records of the southeast Asian paleomonsoons for the last 25 thousand years. Earth Planet Sci Lett, 1997, 146: 59－72
22 Shackleton N J. The 100,000-year ice-age cycle identified and found to lag temperature, carbon dioxide, and orbital eccentricity. Science, 2000, 289: 1897－1902
23 Li J R, Carbon reservoir in low-latitude oceans and orbital cycles of monsoon climate (in Chinese). Dissertation for the Doctoral Degree. School of Ocean and Earth Science. Shanghai: Tongji University, 2007
24 Müller P J, Kirst G, Ruhland G, et al. Calibration of the alkenone paleotemperature index $U^{k'}_{37}$ based on core-tops from the eastern South Atlantic and the global ocean (60°N－60°S). Geochim Cosmochim Ac, 1998, 62: 1757－1772
25 Villanueva J, Flores J A, Grimalt J O. A detailed comparison of the Uk037 and coccolith records over the past 290 kyears: implications to the alkenone paleotemperature method. Org Geochem, 2002, 33: 897－905
26 Levitus S, Boyer T. NOAA Atlas NESDIS vl4: Temperature. World Ocean Atlas 4, U.S. Department of Commerce, Washington D C, 1994
27 Pelejero C, Calvo E, Barrows T T, et al. South Tasman Sea alkenone paleothermometry over the last four glacial/interglacial cycles. Mar Geol, 2006, 230: 73－86
28 Lea D W, Pak D K, Spero H J. Climate impact of late Quaternary equatorial Pacific sea surface temperature variations. Science, 2000, 289: 1719－1724
29 Emeis K-C, Anderson D M, Doose H, et al. Sea-surface temperatures and history of monsoon upwelling in the northwest Arabian Sea during the last 500000 years. Quat Res, 1995, 43: 355－361
30 Pahnke K., Zahn R., Elderfield H, et al. 340000-year centennial-scale marine record of Southern Hemisphere climatic oscillation. Science, 2003, 3001: 948－952
31 Herbert T D, Schuffert J D, Andreasen D, et al. Collapse of the California Current during glacial maxima linked to climate change on land. Science, 2002, 293: 71－76
32 Visser K, Thunell R C, Stott L. Magnitude and timing of temperature change in the Indo-Pacific warm pool during deglaciation. Nature, 2003, 421: 152－155
33 Rosenthal Y, Oppo D W, Linsley B K. The amplitude and phasing of climate change during the last deglaciation in the Sulu Sea, western equatorial Pacific. Geophys Res Lett, 2003, 30, doi:10.1029/2002GL016612
34 Luo Y L, Sun X J, 2005, Vegetation evolution and millennial-scale climatic fluctuation since Last Glacial Maximum in pollen record from northern South China Sea. Chinese Sci Bull, 2005, 50: 793－799
35 Wang W Y, Liu J Q, Negendank J, et al, The two-step monsoon changes of the last deglaciation recorded in tropical Maar Lake Huguangyan, southern China. Chinese Sci Bull, 2000, 45: 1529－1532
36 Stott L, Poulsen C, Lund S, et al. Super ENSO and global climate oscillations at millennial time scales. Science, 2002, 297: 222－226
37 Koutavas A, Lynch-Stieglitz J, Marchitto T, et al. El Niño-like pattern in ice age tropical Pacific sea surface temperature. Science, 2002, 297: 226－230
38 Li L, Wang H, Li J R, et al. Variability of sea surface residual oxygen isotopic and salinity in western south china sea over late Pleistocene (in Chinese). Quat Sci, 2008, 28: 399－406
39 Kiefer T, Kienast M. Patterns of deglacial warming in the Pacific Ocean: a review with emphasis on the time interval of Heinrich event 1. Quat Sci Rev, 2005, 24: 1063－1081
40 Bard E. Comparison of alkenone estimates with other paleotemperature proxies. Geochem Geophys Geosy, 2001. 2, 2000GC000050: 1－12
41 Jian Z, Huang B, Lin H, et al. Late Quaternary upwelling intensity and East Asian monsoon forcing in the South China Sea. Quat Res, 2001, 55: 363－370
42 Pflaumann U, Jian Z M. Modern distribution patterns of planktons foraminiferal in the South China Sea and western Pacific: a new transfer technique to estimate regional sea surface temperature. Mar Geol, 1999, 156: 41－83
43 Sikes E L, Keigwin L D. Equatorial Atlantic sea surface temperature for the last 30 ka: A comparison of $U^{k'}_{37}$, $\delta^{18}$O and foraminizferal assemblage temperature estimates. Paleoceanography, 1994, 9: 31－45
44 Conte M H, Eglinton G, Madureira L A S. Long-chain alkenones and alkyl alkenoates as palaeotemperature indicators: their production, flux and early sedimentary diagenesis in the Eastern North Atlantic. Org Geochem, 1992, 19: 287－298
45 Chapman M R, Shackleton N J, Zhao M X, et al. Faunal and alkenone reconstructions of subtropical North Atlantic surface hydrography and paleotemperature over the past 28 ky. Paleoceanography, 1996, 11: 343－358
46 Gong Q J, Wu L J, Wu Sh G, et al. Detection of long chain alkenone compounds and applicationof values in South China Sea (in Chinese). Geochimica, 1999, 28: 51－57
47 Lu B, Chen R H, Fen X W, et al. Study on the paleotemperature, paleoenvironment and biomarker compounds in sediment from the Okinawa Trough during the last 20000 years (in Chinese). Donghai Mar Sci, 2000, 18: 25－32
48 Ijiri A, Wang L, Oba T, et al. Paleoenvironmental changes in the northern area of the East China Sea during the past 42000 years. Palaeogeogr Palaeoclimatol Palaeoecol, 2005, 219: 239－261
49 Zhou H Y, Li T G, Jia G D, et al. Sea surface temperature reconstruction with long chain unsaturated alkenones for the middle okinawa trough during the last glacial-interglacial cycle (in Chinese). Oceanol ET Limnol Sin, 2007, 38: 438－445
50 Benthien A, Müller P J. Anomalously low alkenone temperatures caused by lateral particle and sediment transport in the Malvinas Current region, western Argentine Basin. Deep-Sea Res Pt I, 2000, 47: 2369－2393
51 EPICA Community Members: Augustin L, Barbante C, Barnes PRF, et al. Eight glacial cycles from an Antarctic ice core. Nature, 2004, 429: 623－628
52 McManus J F, Oppo D W, Cullen J L. 0.5 million years of millennial-scale climate variability in the North Atlantic. Science, 1999, 283: 971－975
53 Martrat B, Grimalt J O, Shackleton N J, et al. Four climate cycles of recurring deep and surface water destabilizations on the Iberian Margin. Science, 2007, 317: 502－507
54 Pahnke K, Zahn R. Southern Hemisphere water mass conversion linked with North Atlantic climate variability. Science, 2005, 307: 1741－1746
55 Dannenmann S, Linsley B K, Oppo D W, et al. East Asian monsoon forcing of suborbital variability in the Sulu Sea during Marine Isotope Stage 3: link to Northern Hemisphere climate. Geochem Geophys Geosy, 2003, 4:doi:10.1029/2002GC000390
56 Wang P X. Orbital forcing of the low-latitude processes (in Chinese). Quat Sci, 2006, 26: 694－701
57 Schulz M, Mudelsee M. REDFIT: Estimating red-noise spectra directly from unevenly spaced paleoclimatic time series. Comput Geosci, 2002, 28: 421－426